Journal of Hydrology 638 (2024) 131546

Contents lists available at ScienceDirect

Journal of Hydrology

journal homepage: www.elsevier.com/locate/jhydrol

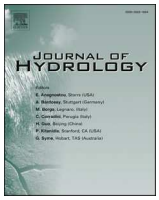

Research papers

Assessment of hydrological parameter uncertainty versus climate projection spread on urban streamflow and floods

Zia Ul Hassan [a,*], Anne J. Jefferson [a,b], Pedro M. Avellaneda [c,d], Aditi S. Bhaskar [e]

[a] Department of Earth Sciences, Kent State University, Kent, OH, USA
[b] Now at: Rubenstein School of Environment and Natural Resources, University of Vermont, Burlington, VT, USA
[c] School of Public and Environmental Affairs, Indiana University, Bloomington, IN, USA
[d] [e]Now at: Environmental Scientist, Clean Water Program, San Francisco Estuary Institute, 4911 Central Ave., Richmond, CA 94804
[e] Department of Civil, Environmental and Architectural Engineering, University of Colorado, Boulder, USA

ARTICLE INFO

This manuscript was handled by Sally Elizabeth Thompson, Editor-in-Chief, with the assistance of Kyle Blount, Associate Editor

Keywords:
Climate change
Bayesian calibration
Uncertainty
Streamflow
Flood frequency
Regional Climate Models

ABSTRACT

Assessing the uncertainty associated with projections of climate change impacts on hydrological processes can be challenging due to multiple sources of uncertainties within and between climate and hydrological models. Here we compare the effects of parameter uncertainty in a hydrological model to inter-model spread from climate projections on hydrological projections of urban streamflow in response to climate change. Four hourly climate model outputs from the RCP8.5 scenario were used as inputs to a distributed hydrologic model (SWMM) calibrated using a Bayesian approach to summarize uncertainty intervals for both model parameters and streamflow predictions. Continuous simulation of 100 years of streamflow generated 90 % prediction intervals for selected exceedance probabilities and flood frequencies prediction intervals from single climate models were compared to the inter climate model spread resulting from a single calibration of the SWMM model. There will be an increase in future flows with exceedance probabilities of 0.5 %-50 % and 2-year floods for all climate projections and all 21st century periods, for the modeled Ohio (USA) watershed. Floods with return periods of $\geq$ 5 years increase relative to the historical from mid-century (2046–2070) for most climate projections and parameter sets. Across the four climate models, the 90th percentile increase in flows and floods ranges from 17-108 % and 11–63 % respectively. Using multiple calibration parameter sets and climate projections helped capture the most likely hydrologic outcomes, as well as upper and lower bounds of future predictions. For this watershed, hydrological model parameter uncertainty was large relative to inter climate model spread, for near term moderate to high flows and for many flood frequencies. The uncertainty quantification and comparison approach developed here may be helpful in decision-making and design of engineering infrastructure in urban watersheds.

1. Introduction

The climatic conditions that drive streamflow are changing worldwide, including rapid increases in intensity and frequency of extreme precipitation events and shifting form and timing of precipitation (Pyke et al., 2011; Voskamp and Van de Ven, 2015). A growing majority of the world population lives in cities (Voskamp and Van de Ven, 2015) and urban areas are more vulnerable than rural to climate change impacts (Revi et al., 2014; Rosenzweig et al., 2019). Intensification of precipitation due to climate change increases runoff from urban impervious surfaces which are hydrologically connected to waterways and causes more severe and widespread flooding in urban areas. The combined consequences of urbanization and precipitation intensification that increase high streamflows and flooding could lead to poor water quality of receiving water bodies (Wang et al., 2017), increases in erosion from streambeds and banks, and deterioration of the urban ecological environment (Pyke et al., 2011). Neighborhood flooding and infrastructure failure can result if existing drainage systems are not sufficient to handle increasing high flows (O'Donnell and Thorne, 2020; Zhou et al., 2019).

Increases in extreme rainfall across the United States require modifications to existing hydrological design standards to account for climate change (Wright et al., 2021, 2019). The consequences of ignoring uncertainties associated with climate change projections could lead to over-design or under-design of water infrastructure (e.g., Cook et al., 2020). Over-design can be costly, and under-design could lead to risk of failure (Kim et al., 2019). Considering uncertainties during forecasting

* Corresponding author.
E-mail address: zhassan1@kent.edu (Z. Ul Hassan).

https://doi.org/10.1016/j.jhydrol.2024.131546
Received 22 April 2023; Received in revised form 19 May 2024; Accepted 5 June 2024
Available online 17 June 2024

of future hydrological variables can be helpful for decision makers and user groups to make robust and more sustainable decisions to achieve higher level of confidence during climate change adaptations (Krysanova et al., 2018).

A major challenge for understanding how climate change will impact urban hydrology is the cascading uncertainty associated with climate projections and hydrological modeling. Uncertainties in regional climate change projections can be due to choice of emissions scenarios, structure, parameterization, and resolution of climate models, and bias correction approach (Kundzewicz et al., 2018). Using hydrological models to understand climate change impacts brings additional sources of uncertainties, which are related to model representation of hydrologic processes, assumptions, spatial and temporal discretization, availability of data, computational resources, and calibration techniques (Joseph et al., 2018; Mendoza et al., 2015). There is rich literature on uncertainty estimation in both climate science and hydrology (e.g., Feng and Beighley, 2020; Liu and Gupta, 2007; Steinschneider et al., 2012), and at their intersection in non-urban catchments (e.g., Bosshard et al., 2013; Chegwidden et al., 2019; Clark et al., 2016). There has been comparatively little work on uncertainty applied to understanding the hydrological impacts of climate change in urban catchments (Lai et al., 2022). Jung et al., (2011) considered uncertainties in the projections of future flood frequencies in urban watersheds using the Precipitation Runoff Modeling System (PRMS) and found that climate model uncertainties were larger than hydrological model parameter uncertainties. However, PRMS does not represent the stormwater pipe network or connectivity of impervious surfaces, which are important determinants of urban hydrologic response (Meierdiercks et al., 2010; Sytsma et al., 2020).

Parameter uncertainty is a significant source of uncertainty in complex urban hydrological models that represent pipe flow and impervious connectivity, like the popular Stormwater Management model (SWMM) (e.g., Li et al., 2016; Avellaneda et al., 2017). These features introduce parameters, such as imperviousness, depression storage on impervious surfaces, and sub catchment characteristic width, to which model performance is sensitive (e.g., Barco et al., 2008; Perin et al., 2020; Shahed Behrouz et al., 2020). Recent work has also identified the issue of calibration transfer parameter uncertainty in semi-distributed models like SWMM, when the optimal effective model parameters change with model forcing, including climate changes (Systma et al., 2022). Parameter uncertainties can be determined by using Monte Carlo simulations to generate parameter combinations that produce acceptable model performance (Beven, 2009; Deletic et al., 2012). Bayesian modeling approaches embrace multiple equally acceptable calibration parameters for the quantification of uncertainties associated with calibration parameters in SWMM or other models (Avellaneda et al., 2017; Muleta et al., 2013; Zahmatkesh et al., 2015). Further, modeling studies of climate change impacts on urban streamflow mostly use event-based calibration and focus on design storms for analysis (e.g., Alamdari et al., 2017; Wang et al., 2019), rather than focusing on continuous discharge simulations where antecedent conditions may have an influence. Bayesian modeling approaches, combined with continuous simulations, present a pathway to evaluate the effects of hydrologic parameter uncertainty in models that represent urban infrastructure, versus the uncertainty arising from climate models.

Both the magnitude and type of climate change and the consequent hydrological response are region specific (Hayhoe et al., 2008; Joseph et al., 2018; Naz et al., 2016). The US Midwestern and Great Lakes region is expected to be substantially affected by increasing temperature and precipitation through the 21st century (Byun and Hamlet, 2018; Chien et al., 2013; Sharma et al., 2018), resulting in changes to streamflow. Increasing hydrological extremes, especially flooding, are creating regional challenges for water management infrastructure, including urban stormwater conveyance systems (Wilson et al., 2023; Olds et al., 2018). Future climate change is projected to increase these stormwater challenges (e.g., Moore et al., 2016). However, previous studies that evaluate the impact of climate change in Midwest on hydrological extremes have not focused on urban streamflow, leaving an information gap for urban watershed managers.

The goal of this research is to consider the effects of parameter uncertainty in hydrologic modeling versus spread among a climate model ensemble on projected changes in urban streamflow and floods for a typical urban watershed in the US Great Lakes region. Despite additional parameters required to represent urban watersheds, we hypothesized that uncertainty associated with using multiple climate models would be larger than the parameter uncertainties associated with SWMM hydrologic model calibration for the projection of flow duration curves and flood frequencies in an urban watershed, based on studies in non-urban watersheds (e.g., Chegwidden et al., 2019; Clark et al., 2016). In a novel approach, we used a Bayesian calibration to incorporate uncertainties associated with calibration parameters in SWMM and compared them to the spread arising from four hourly climate model outputs in continuous simulations of 100 years of streamflow. The approach used in this research work helped identify and quantify uncertainties between multiple climate projections and within urban hydrological model parameterization across a wide range of flows, providing guidance for future efforts to design infrastructure in the context of uncertainty.

2. Materials and methods

2.1. Study area and model structure

The 20.63 km^2, 30.3 % impervious West Creek watershed is typical of suburban-urban watersheds in the Cleveland metropolitan area of northeast Ohio, USA (Fig. 1). The Cleveland Hopkins International Airport, located 13 km to the west of the West Creek watershed has normal (1991–2020) mean annual precipitation of 1042 mm, mean annual temperature of 11.3 °C, and it receives snowfall during the months of November to April. West Creek, with a length of 14.4 km, drains into the Cuyahoga River and ultimately, Lake Erie. The stormwater pipe network in the watershed is separate from the sanitary sewerage network and stormwater drains into West Creek at multiple locations. Low to moderate hydraulic conductivity of soils in West Creek allow some infiltration but these soils combined with impervious surfaces, also quickly drain runoff into drainage infrastructure, where it ends up in the stream (Cuyahoga County Planning Commission, 2001). Previously, subwatershed-scale paired watershed studies (Avellaneda et al., 2017; Jarden et al., 2016; Turner et al., 2016) and watershed-scale SWAT modeling (Avellaneda and Jefferson, 2020) have been used in the West Creek watershed to examine the impact of green infrastructure on streamflow, but these studies did not explore the effects of climate change.

A distributed stormwater management model (SWMM5.1.015) was used to simulate streamflow at the watershed outlet (Rossman, 2010). Initial development of the SWMM model for West Creek was done by Northeast Ohio Regional Sewer District (NEORSD), and the model was modified and calibrated in this study. The watershed was divided into 94 smaller sub-watersheds and water from the subwatersheds drains into the stream channel network. In the SWMM model, the stormwater management infrastructure consists of one storage node representing a 1.25 ha dam pond, 236 conduits (including pipes and the open channel network) with a total length of 18.14 km, and 219 junctions.

SWMM uses a mass balance approach for the simulation of watershed hydrology, while the routing of flow in pipes and channels is done by the Saint Venant equation. Time series of precipitation, temperature, and evapotranspiration serve as inputs to simulate streamflow in SWMM. Potential evapotranspiration was calculated using the Penman-Monteith equation separately, following the American Society of Civil Engineers (ASCE) manual Allen et al., (2005), and then included as an input series. A modified Green-Ampt equation was used for the estimation of infiltration. The modeling of stream baseflow was done with the help of the groundwater module in the SWMM model. SWMM considers and analyzes the base flow separately for each subwatershed (Rossman, 2010).

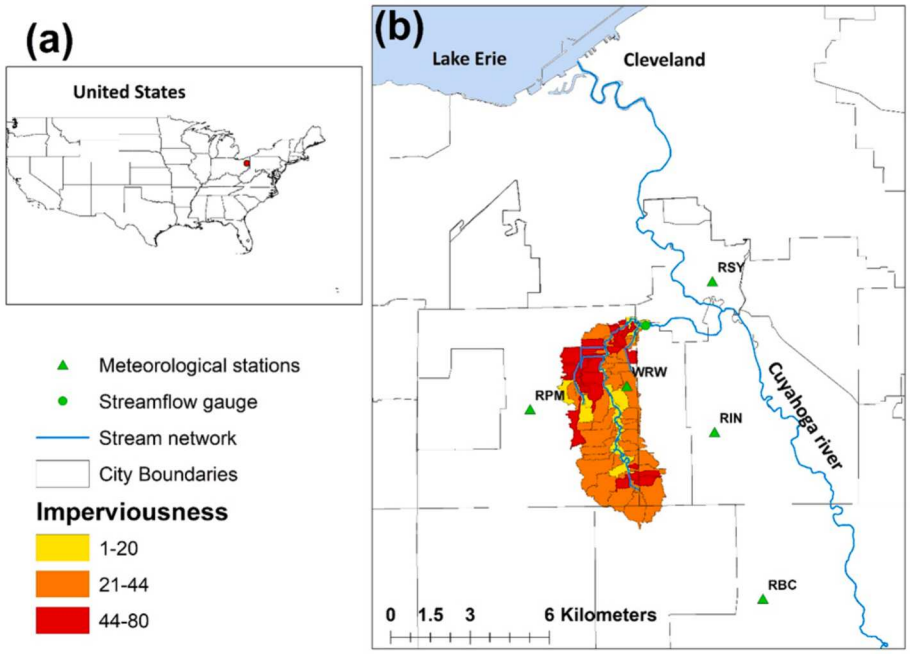

Fig. 1. The West Creek watershed in (A) the United States, with the red dot representing the location of West Creek and (B) context of its SWMM subwatershed (gray borders), subwatershed imperviousness (colors), stream network (blue line), and surrounding meteorological stations (green triangles). (For interpretation of the references to colour in this figure legend, the reader is referred to the web version of this article.)

The dynamic wave routing method with a routing step of 30 s was used in this study for the simulation of flow. The routing step was chosen using a manual optimization of performance and simulation time.

2.2. Climate and streamflow data

For model calibration, precipitation data for 2013 through 2019 with a temporal frequency of 5 min from four meteorological stations surrounding the watershed was provided by Northeast Ohio Regional Sewer District (NEORSD). Four meteorological stations were used for calibration to capture the spatial variability of precipitation across the watershed and fill missing data. The percentage of missing data for each station was < 1 %. Missing data were filled by linear regression between the datasets and data from the West Ridgewood meteorological station operated by Cleveland Metroparks, located within the West Creek watershed. Thiessen polygons were used to create a single precipitation time series for hydrologic model calibration (section 2.4). Streamflow data at 5-minute intervals from 2013 to 2019 was obtained from the U.S. Geological Survey (USGS 412453081395500) station located near the outlet of West Creek at Brooklyn Heights, Ohio. The percentage of missing data for streamflow ranges from 5-15 % per year, and missing data were excluded from calibration statistics.

Modeled future temperature data that is required to calculate evapotranspiration and precipitation were extracted from the North American Coordinated Regional Climate Downscaling Experiment (NA-CORDEX), with a spatial resolution of 0.22°/25 km and temporal resolution of one hour (Mearns et al., 2009, Mearns et al., 2017). This spatial and temporal resolution represents the finest climate model resolution publicly available at the time of the study. The NA-CORDEX time series are generated from dynamically downscaled regional climate models (RCMs) with differing parent global climate models (GCMs) forced by the RCP8.5 emission scenario. All four climate model outputs with one hour time step data available through NA-CORDEX in May 2020 were used in this analysis. These outputs are: (1) RegCM4 with parent GCM MPI-ESM-LR (hereafter "RegCM4_MPI-ESM-LR"), (2) WRF with parent GCM GFDL-ESM2M ("WRF_GFDL-ESM2M"), (3) WRF with parent GCM HadGEM2-ES ("WRF_HadGEM2-ES"), and (4) WRF with parent GCM MPI-ESM-LR ("WRF_MPI-ESM-LR"). The data were divided into four different periods historical (1976–2000), initial (2021–2045), mid (2046–2070), and late century (2071–2095). For bias correction, hourly historical data for 1976 through 2000 from Cleveland Hopkins International Airport (CLE) were obtained from the Iowa Environmental Mesonet database (https://mesonet.agron.iastate.edu/climate/). The historical temperature, relative humidity, wind speed, solar radiation and atmospheric pressure datasets required to calculate evapotranspiration were missing 0.42 %, 0.60 %, 0.50 %, 5.16 % and 0.3 % of observations, respectively. A mixture of future and historical climatic data were used to calculate future evapotranspiration because NA-CORDEX RCMs only provide future precipitation and temperature data.

2.3. Bias correction and disaggregation of RCM outputs

Bias correction is an important step for the postprocessing of RCM output for use in climate change projections, because it can remove biases including errors due to the imperfect parameters used for climate simulations and imperfect boundary conditions provided by a GCM (Chen et al., 2013). There are many different methods available for bias correction, ranging from simple scaling techniques to more advanced distribution mapping techniques (Luo et al., 2018). The quantile mapping approach was used here, because Chen et al., (2013) found this distribution-based bias correction technique was most useful for the North American region. Adjustments made using this method are based on large scale distribution of RCM outputs (P_s) with the observed time series known as reference time series (P_o) using a transform function (h) (Aslam et al., 2020; Chen et al., 2013). The equation for the quantile mapping approach can be written as:

$$P_o = h(P_s) \tag{1}$$

The transformation for the known distribution of variable of interest is defined in the equation below:

$$P_o = F_o^{-1}(F_s(P_s)) \tag{2}$$

where Fs represents the Cumulative Distribution Function (CDF) of P_s

and F_o^{-1} represents the inverse of CDF of P_o. Bias corrections identified for the historical (1976–2000) RCM data, using the observed hourly precipitation and temperature data at Cleveland Hopkins International Airport, were applied to RCM projections of future temperature and precipitation. The bias correction of temperature and precipitation were performed separately on each time series, so the two series may not match in terms of weather pattern timing. Depth-duration-frequency analysis was performed on bias-corrected precipitation data using generalized extreme value function fitting using the L-moments method. Depth-duration-frequency analysis was performed for 1-hour and 24-hour storms and 5 different recurrence intervals (6-months, 1-year, 2-year, 5-year and 10-year).

Previous efforts to model the hydrology of West Creek at hourly timesteps have underestimated peak flows (Avellaneda and Jefferson, 2020), so disaggregation of bias-corrected hourly RCM precipitation data to 5-minute intervals was used to improve the hydrologic model performance of urban streamflow dynamics. The NetSTORM model (Heineman, 2012) was used for disaggregation of RCM precipitation data from hourly to 5-minute timesteps. NetSTORM modifies a previous empirical stochastic disaggregation method (Ormsbee, 1989) by adding a spiking factor to improve performance and increase intensities at the 5-minute timescale. A spiking factor of 0.5 and pulse depth of 0.01 was used in this research, with spiking factor and pulse depth adjusted by manual calibration.

2.4. Hydrologic model calibration and validation

Selection of 16 parameters for calibration (Table 1) was based on sensitivity analysis using the sensitivity-based ratio tuning calibration tool (SRTC) available in PCSWMM (Computational Hydraulics International, Guelph, ON) and existing literature (Shahed Behrouz et al., 2020). The SRTC tool consists of radio sliders that are helpful in changing parameters within the defined range to match the simulated streamflow with observed streamflow. Calibration and validation of five parameters for snow melt and groundwater were done manually against snow water equivalent data from the Cleveland airport and streamflow data from USGS gauge respectively.

An informal likelihood function (i.e., Nash and Sutcliffe efficiency with shaping factor) available in the Differential Evolution Adaptive Metropolis (DREAM) algorithm was used for the uncertainty-based calibration (Freer et al., 1996; Vrugt, 2016) to find an optimal set of 11 parameters that are equally acceptable as simulators of a watershed's hydrology. (Schoups and Vrugt, 2010) tested the DREAM algorithm for the calibration of a simple conceptual rainfall-runoff hydrological model. This uncertainty-based calibration was used for six surface water parameters (related to imperviousness, roughness, depression storage, and width); three infiltration parameters; and two groundwater parameters (Table 1). Limits for parameter ranges explored during calibration were identified from the literature (e.g., Shahed Behrouz et al., 2020). The imperviousness and width parameters varied among the subcatchments based on subcatchment characteristics in the initial model. These two parameters were calibrated in the DREAM algorithm based on the percentage change from initial values. All other parameters were uniform across subcatchments.

Table 1
Parameters used for calibration of the SWMM model. The limits for calibration of width and imperviousness represent the proportional change from the values for each subwatershed in the uncalibrated model.

Parameters	Calibration Method	Representation	Limits for Calibration
Imperviousness (−)	DREAM	Surface water	−0.3–0.3
Width (−)	DREAM	Surface water	−0.3–0.3
N-Imperviousness (−)	DREAM	Surface water	0.01–0.02
N-Perviousness (−)	DREAM	Surface water	0.01–0.4
S-Imperviousness (in)	DREAM	Surface water	0–3
S-Perviousness (in)	DREAM	Surface water	0–3
Suction Head (in)	DREAM	Infiltration	0–10
Hydraulic Conductivity (in/hr)	DREAM	Infiltration	0–1
IMD max (−)	DREAM	Infiltration	0.1–0.4
A1 (−)	DREAM	Groundwater	0–0.5
B1 (−)	DREAM	Groundwater	0–3
Lower Groundwater loss rate (−)	Manual	Groundwater	0.005–0.01
Unsaturated soil zone moisture(fraction)	Manual	Groundwater	0.25–0.35
Minimum Melt Coefficient (−)	Manual	Snow Melt	0.0005–0.001
Maximum Melt Coefficient (−)	Manual	Snow Melt	0.001–0.0017
Base Temperature (F)	Manual	Snow Melt	29.5–31.5

The summation of the squared errors as the basic likelihood measure was used in this study for the computation of results (Freer et al., 1996). This measure is

$$L(\theta_i|\,Q_{obs}) = Glog\left(1 - \frac{\sum_{t=1}^{T}\left(Q_{obs,t} - Q_{sim,i}\right)^2}{\sum_{t=1}^{T}\left(Q_{obs,t} - \overline{Q_{obs}}\right)^2}\right) \quad (3)$$

where L is the likelihood function of the i^{th} parameter set conditioned on the observed discharge Q_{obs}, θ_i represents a set of model parameters, $Q_{obs,t}$ represents observed discharge at time t, $Q_{sim,i}$ represents the simulated discharge at time t and is a function of θ_i , $\underline{Q_{obs}}$ is the mean of the observed discharge, T is the total time, and G is a shaping factor. We have used a value of 10 for the shaping factor (Vrugt, 2016).

An acceptance rate greater than 15 % and $\widehat{R} < 1.2$ for all parameters used for calibration is a good indicator of acceptable performance and convergence (Vrugt, 2016). $\widehat{R}$ is a statistic to determine when convergence of the sampled Markov chains has been achieved. The DREAM algorithm can calculate the acceptance rate and $\widehat{R}$ automatically for each chain during simulations. During the calibration phase, DREAM converged successfully within 10,000 simulations. After DREAM converged, a subset of 224 parameter sets were chosen based on acceptable values for the acceptance rate and available computing resources (8 cores with 28 cores per node; 8x28 = 224).

The median of streamflow from 224 calibration parameter sets simulations has been used to compare with observed flow for both calibration and validation years. Water year 2017 data were used for calibration, because it was not unusually wet or dry relative to the available record. Water years 2015–2016 and 2018–2019 were used for model validation. Water year 2014 data were also used as a one-year hot start in the SWMM model to stabilize initial conditions. The performance of the calibrated model was calculated by using percentage coverage (observations falling within 95 % prediction intervals), Nash-Sutcliffe efficiency coefficient (NSE), and coefficient of determination (R^2).

2.5. Streamflow analysis

Once calibrated and validated, the SWMM model was used to simulate streamflow for one period with historical RCM data (1976–2000) and three future periods (2021–2095) for all four climate model outputs using each of the 224 sampled parameter sets, to capture the uncertainties associated with calibration parameters and variability across climate models. Streamflow metrics were calculated from discharge time −series from the 224 sampled parameter sets.

Flow duration curves were constructed using the simulated streamflow time series from exceedance probability (P) of ranked streamflow data, using

$$P = [M/(n+1)\,] \quad (4)$$

where, M represents the ranked position from highest to lowest and n represents the total number of values in the streamflow time series. Flow duration curves were calculated for each period and flows at different

exceedance probabilities (0.5 %, 10 %, 25 %, 50 %) were extracted from flow duration curves to calculate the percentage change as compared to the historical period. Low flows with an exceedance probability greater than 50 % were not used in further analysis, due to the limitations of calibration for low flows using the SWMM model (Avellaneda et al., 2017; Hamel et al., 2013; Hossain et al., 2019; Nayeb Yazdi et al., 2019). Flow duration curves were also calculated on a seasonal basis for summer (June-August), winter (December-February), spring (March-May), fall (September-November).

The Gumbel distribution was used to estimate flood frequencies of different return periods (2, 5, 10, 25, 50, 100 years) using the annual maximum 5-minute streamflow for each climate model output, analysis period, and parameter set. The Gumbel distribution has been extensively used in previous studies for the estimation of flood frequencies e.g., (Alfieri et al., 2015; Pang et al., 2022).

We selected a single, representative parameterization of the SWMM model to use for quantification of the effects of inter-climate model spread on hydrologic projections. As our representative parameterization, we identified the single parameter set that produced the flow duration curve closest to the median streamflow at each quantile from all parameter sets, as measured by least value of root mean square error relative to the median streamflow. This was done separately for the historical period for each RCM and resulted in identification of the same parameter set for all climate model outputs (hereafter, the median parameter set). Note that the median parameter set may not produce the median of the cumulative distribution function (CDF) for specific flow return periods (Fig. 2). The median parameter set thus represents one realization of calibration for each climate model output (black dots in Fig. 2). Observing the range of these parameter sets (black horizontal lines in Fig. 2) allows us to assess the inter-climate model spread. In addition, the uncertainties associated with the hydrologic model parameterization are assessed through the 90 % prediction intervals (PI) of the CDF curves produced from each of the four climate models with the 224 parameter sets for the selected exceedance probabilities and flood frequencies (PIs shown as colored horizontal lines in Fig. 2). To summarize, the inter-climate model spread was assessed through the range of median parameter sets (width of black line, Fig. 2), while the hydrologic parameter uncertainty was assessed by the widths of all four PIs (colored lines, Fig. 2). If all four PIs are larger than the range of median parameter sets, we conclude that hydrological parameter uncertainty is more important than climate model spread (for example, Fig. 2a, all four colored line widths are larger than black line). Conversely, if the range of median parameter sets is larger than all four PIs, we conclude that climate model spread is more important than hydrological parameter uncertainty (for example, Fig. 2b, black line width is larger than all four colored lines). Finally, if the range of median parameter sets is smaller than some of the PIs but larger than others, we interpret this result to mean both uncertainties are approximately equally important (for example, Fig. 2c, black line is smaller than brown and green lines, but larger than blue and red lines).

3. Results

3.1. Changes in temperature and precipitation

Raw climate model output overestimated total monthly precipitation and underestimated mean monthly temperature as compared to observed data (Fig. S1a-b). Mean absolute error (MAE) between observed and raw hourly precipitation and temperature data ranges from 0.24-0.29 mm and 0.5–0.9 °C respectively. After bias correction, MAE is reduced to 0.20–0.21 mm for precipitation and 0.1–0.2 °C for temperature.

Across the four climate model outputs, bias-corrected mean annual temperature is projected to increase by 1.3–1.9 °C in the initial period, by 2.7–3.7 °C in the mid-century, and by 4.1–6.0 °C in the late century relative to historical temperatures (Table S1). Variation between the climate models in mean annual temperature is less for the historical period and more for the late century (Table S1). Across the four climate models, mean annual precipitation is projected to increase by 136–140 mm during the initial period, 138–340 mm during the mid-century, and 209–445 mm during the late century, relative to the historical period, (Table S2). The maximum increase in mean monthly precipitation occurs in April (Fig. S2).

Depth-duration-frequency curves for 1-hour storms show that there will be an increase in precipitation depth by 14–40 % in the late century relative to the historical period, for 6-month to 10-year return periods (Fig. 3). The range reflects variability across climate models, and all return periods have similar projected percentage increases. Results for the 24-hour storm show somewhat greater increases, with up to a 50 % increase in precipitation from 1- and 2-year storms (Fig. S4).

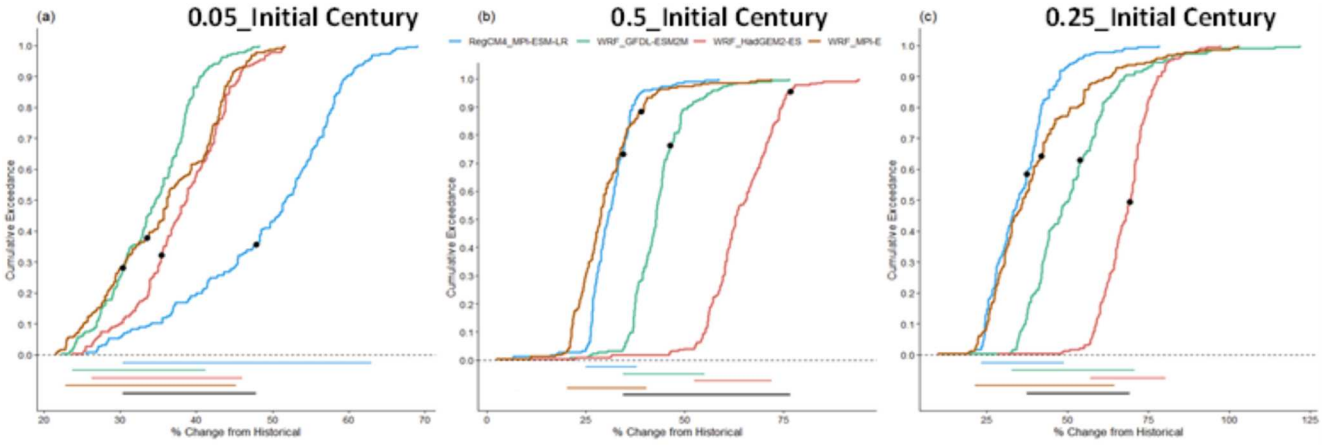

Fig. 2. Illustration of the change from historical conditions for selected flow exceedances produced by 224 hydrological parameter sets per climate model output (colored CDF curves), versus the range of change projected by a single realization (median parameter set, black dots) across climate model outputs. The horizontal lines below the CDFs illustrate the 90% PI for each climate model output (colored lines) and the inter-model spread for the median parameter set (black line). In (a), inter-climate model spread is smaller than all hydrological PIs for flows with an exceedance probabilities of 0.05 for initial century period, indicating that hydrological parameter uncertainty is more important than climate model spread. In (b), inter-climate model spread is larger than all hydrological PIs for an exceedance probabilities of 0.5 for initial century period, indicating that climate model uncertainty is more important than hydrological parameter uncertainty. In (c), inter-climate model spread is larger than some, but not all hydrological PIs, for an exceedance probabilities of 0.25 for initial century period, indicating that climate model and hydrological parameter uncertainty are approximately equal.

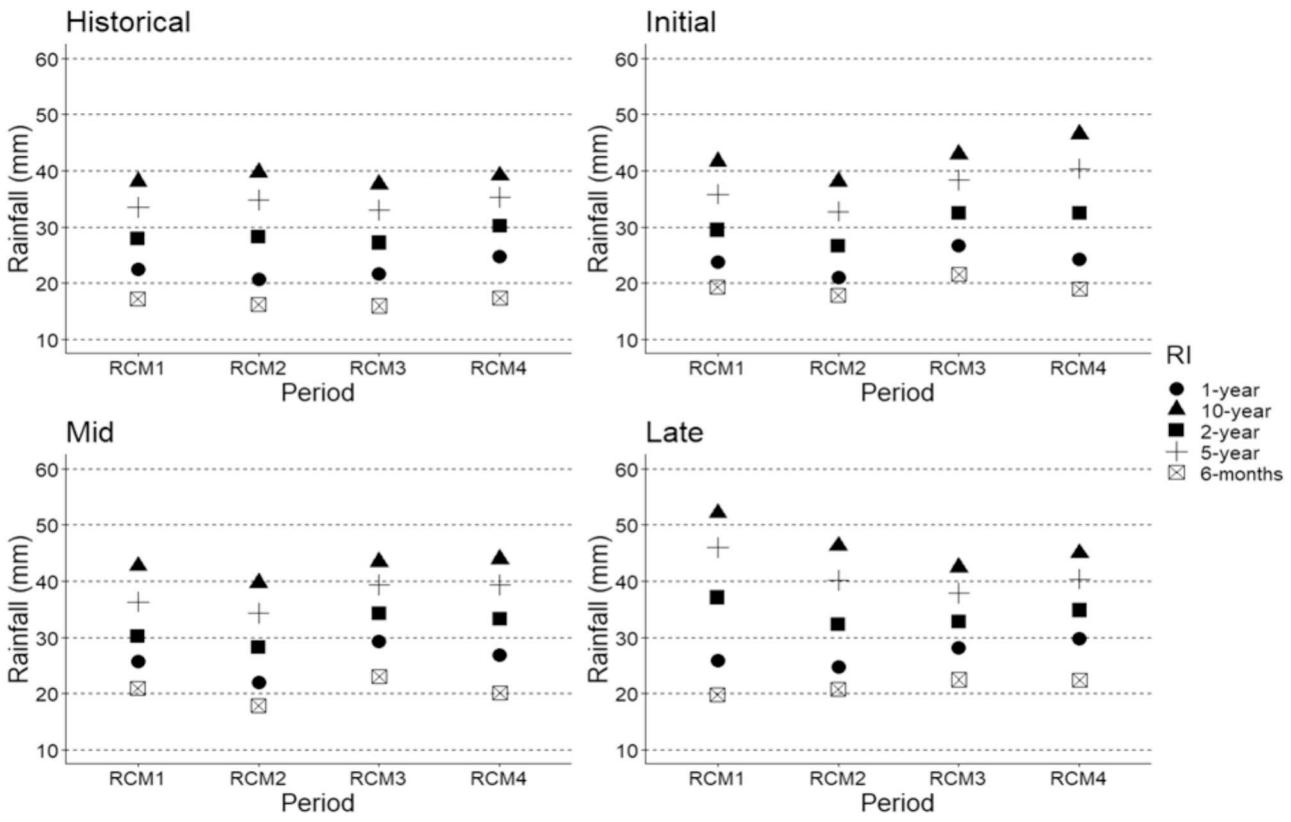

Fig. 3. Results of 1-hour depth-duration-frequency analysis for climate model outputs. The historical period is 1976–2000, initial is 2021–2045, mid is 2046–2070, and late is 2071–2095. RCMs are termed RCM1 (RegCM4 with parent GCM MP1-ESM-LR), RCM2 (WRF with parent GCM GFDL-ESM2M), RCM3 (WRM with parent GCM HadGEM2-ES), RCM4 (WRF with parent GCM MPI-ESM-LR).

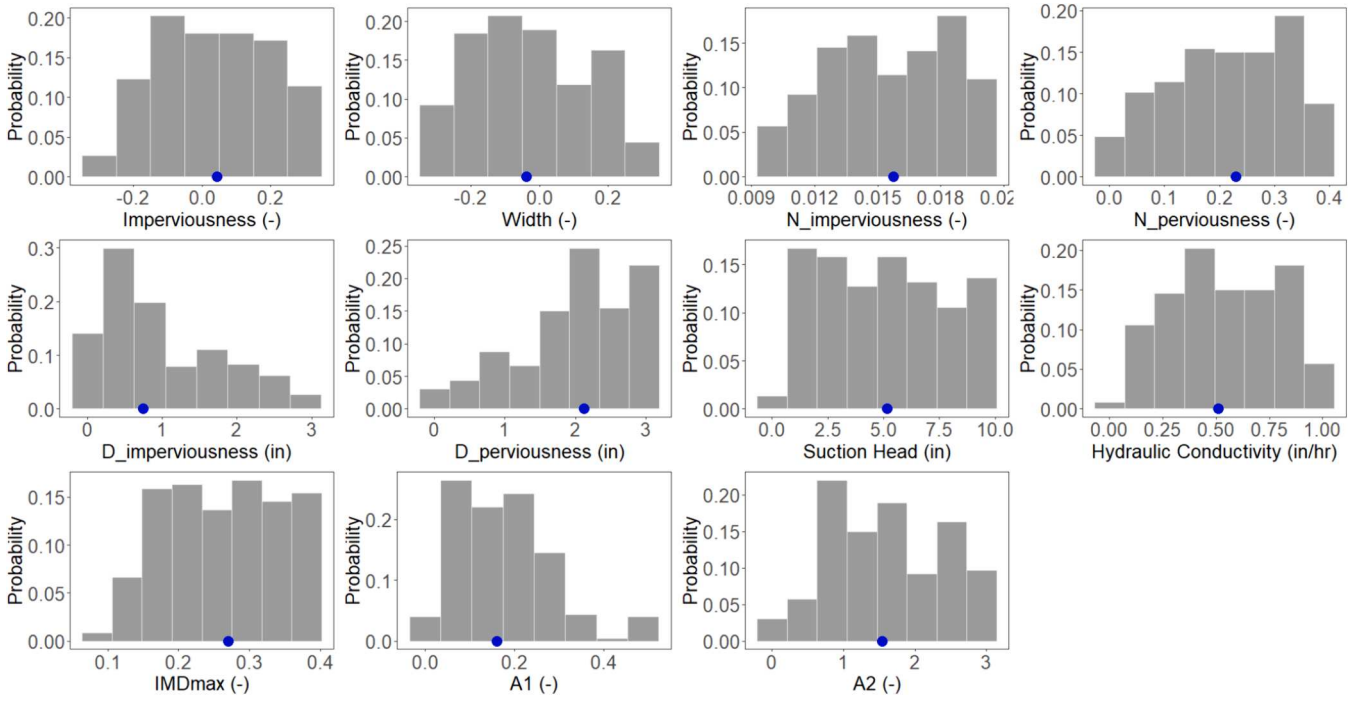

Fig. 4. Probability distribution of parameters used for calibration and validation of PCSWMM model for West Creek. Each distribution is based on 224 sampled parameter sets. The median of each distribution is shown with a blue dot. The values for width and imperviousness represent the proportional change from the values for each subwatershed in the uncalibrated model. (For interpretation of the references to colour in this figure legend, the reader is referred to the web version of this article.)

3.2. Hydrological model performance

91942191688125Probability distributions from the 224 parameter sets sampled after model convergence show distributions around the median parameter values (Fig. 4). The model performs well for high flows and rising and falling limbs of the observed and simulated hydrographs match well with each other (Fig. 5). Comparison between observed and median simulated discharges for four validation years found satisfactory performance in all years, with NSE ranging from 0.62 to 0.74 and R^2 ranging from 0.64 to 0.76 (Table 2). The percent of observations within the simulated 95 % prediction interval (coverage (%) in Table 2) for the years 2014 and 2015 was lower than 50 %, likely because of the higher percentage of low flow periods during those years and the choice of likelihood function for calibration of the model. (Avellaneda et al., 2017) also found less good performance of a SWMM model for low flow periods following calibration using NSE.

Most parameter sets are tightly clustered around the median parameter set over the whole flow duration curve (Figs. S5–S8). There were 8 parameter sets that showed a wide spread in flow duration curves from median, especially for the medium and low flows. The parameter sets showing this dispersion were consistent across climate model outputs. The median and low flows exhibited a wider spread as compared to the high flows.

3.3. Flow duration curves

Climate change increases streamflow in West Creek as compared to the historical period. The median flow duration curves (FDC) (i.e., the FDC generated by the median parameter set) shifts upward in all future periods and in all climate model outputs for flows with $\leq$ 50 % exceedance (Fig. 6). For the 0.5 %, 10 %, 25 %, and 50 % exceedance probability flows, the patterns of hydrological variation among climate model outputs and over time are broadly similar (Fig. 7, Figs. S9-S11). There is more agreement in percentage change of flows across climate models during the initial period as compared to the mid and late periods (Fig. 7).

To understand what information would be lost by considering only a single SWMM calibration for each climate model, we plotted the CDF from all 224 simulations of all four climate models (896 simulations total) and identified the four values that would be identified if only the median parameter set had been used (Fig. 8). For the median (50 % exceedance flow), the four median parameter sets span ~ 60 % of the CDF in the initial period and ~ 80 % of the CDF in the mid and late periods, but the median parameter sets from WRF_HadGEM2-ES is very near the high end of the CDF (67–98 %) for all future periods (Fig. 8a). If only one hydrological simulation were done for each climate model, this result might not be considered an extreme projection of future change. For the 25 %, 10 %, 0.5 % exceedance flows, the four median parameter sets bracket the steep part of the CDF, spanning about 60 % of the total CDF and are reasonably symmetrical around the median (Fig. 8cba). For some flows in some future periods, median parameter sets from two climate models produce very similar results (e.g., 25 % exceedance, mid period). If median parameter sets generate results on the tail of the CDF, and only a single calibration is considered, the likelihood of a large or small change in flow could be over-estimated. For example, for 0.5 % exceedance in the late period (Fig. 8a), two of the median parameter sets produce results that are around 0.2 on the overall CDF, which could lead to over-estimating the probability of a small change in future flows.

For most of the analyzed future flows, climate model spread is more important than parameter uncertainty, based on comparing the range of median parameter sets and the 90 % PI for each model (Fig. 8). Over the 21st century, both climate model spread and PIs increase, but climate model spread increases more quickly. For the initial period, flows with 0.5 % and 10 % exceedance have PIs that are greater than the range across climate models, so parameter uncertainty is more important for the overall uncertainty of those flows (Fig. 8ab). For the 25 % exceedance flow, the two sources of uncertainty are approximately equal (Fig. 8c), whereas for 50 % exceedance flows, climate model variability is more important than the parameter uncertainty (Fig. 8d). During the mid-century period, 0.5 % exceedance flows are approximately equally affected by parameter uncertainty and climate model spread (Fig. 8a), but for the same period, smaller flows are more affected by climate model spread than parameter uncertainty (Fig. 8b-d). During the late century, flows with all exceedance probabilities have climate spread spread greater than the PI range, so climate model uncertainties are more important than parameter uncertainties as we move farther into the future (Fig. 8).

3.4. Flood frequency analysis

The use of multiple climate model outputs and parameter sets provides a range of possible flood frequencies of 2, 5, 10, 25, 50 and 100 return periods for all periods (Fig. 9, S16-S18). All four climate models produce an increase in the 2-year return period for all future periods

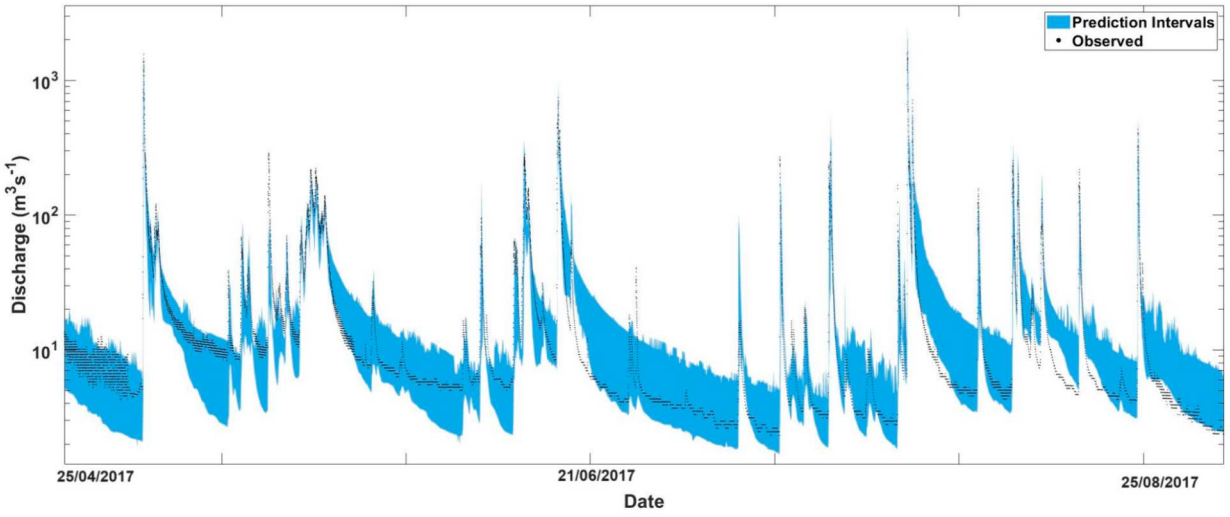

Fig. 5. Simulations of predicted discharge by using 224 sampled parameter sets from DREAM for part of the calibration year (2017). The black dots represent the observations. The blue region represents the 95% predictive uncertainty bounds from discharge simulated by 224 parameter sets. The output time step is 5 min. (For interpretation of the references to colour in this figure legend, the reader is referred to the web version of this article.)

Table 2
Summary of model performance statistics for the median discharge time series and the 224 parameter sets sampled after model convergence.

Water year	Phase	Median Discharge time series			224 Parameter Set Range		
		NSE	R^2	Coverage (%)	NSE	R^2	Coverage (%)
2017	Calibration	0.77	0.78	71	0.64–0.81	0.65–0.84	58–83
2014	Validation	0.67	0.70	23	0.47–0.71	0.58–0.77	18–41
2015	Validation	0.70	0.73	44	0.65–0.73	0.60–0.79	39–55
2016	Validation	0.62	0.64	60	0.57–0.69	0.59–0.72	51–73
2018	Validation	0.74	0.76	49	0.64–0.78	0.71–0.83	45–59

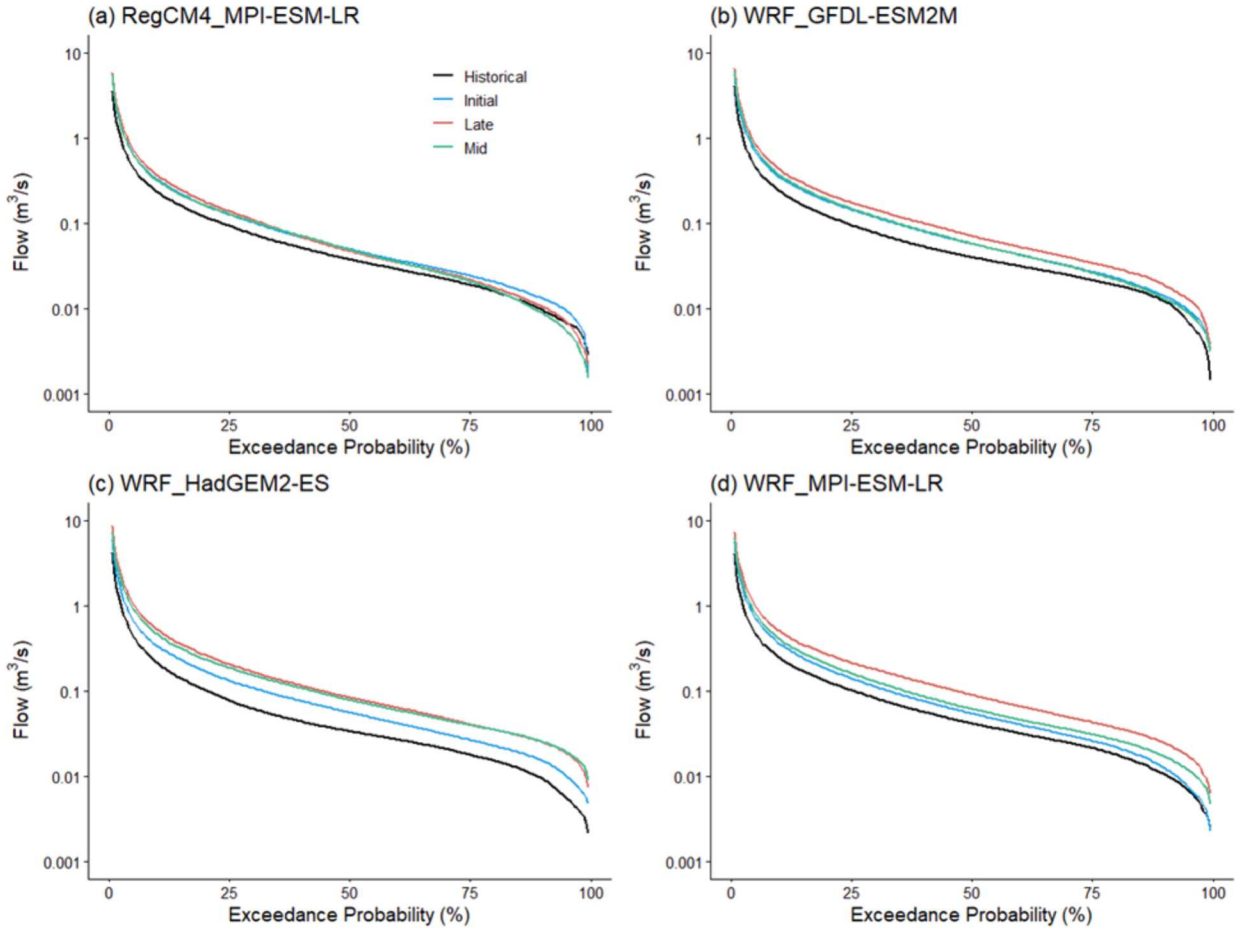

Fig. 6. Flow duration curves for the historical and future periods. Each line represents the curve produced by the median parameter sets, i.e., those that generate the flow duration curve closest to the median for each climate model output in the historical period. The historical period is 1976–2000, initial is 2021–2045, mid is 2046–2070, and late is 2071–2095. In terms of percent change from historical flows, the impact of climate change is larger on the more frequent flows as compared to the 0.5% exceedance flows (Figs. S9-11).

(Fig. 9a), but there is considerable variability among climate models in terms of the ranges of changes. For return periods $\geq$ 5 years, WRF_HadGEM2-ES projects a much smaller change in flood magnitudes than the other climate models (Fig. 9b, Figs. S16 to S19). This difference relative to the other models was not apparent in examination of the precipitation depth-duration-frequency projections (Fig. 3, S3).

Simulations using 224 sampled parameter sets provide a much larger range of future flood predictions than using only the median parameter set for each climate model (Fig. 10). The steepest part of the CDFs of all return periods is well covered by the median parameter sets during the initial and mid periods, with only $\sim$ 20 % and 10 %, respectively, of the largest projected changes not covered by the four median parameter sets. In the late period, however, >40 % of parameter sets produce changes greater than projected by any of the median parameter sets for floods with return periods $\geq$ 5 years. This could lead to under-estimating the true likelihood of large changes, if only one calibration per climate model was used.

For most future floods, parameter uncertainty is approximately equal to or less important than climate model spread, but the importance of parameter uncertainty varies with flood size and the future period (Fig. 10). As flood magnitude increases, climate model spread increases, but the PI remains fairly stable. For the initial period, floods with return periods from 2-25 years have PIs that are both larger and smaller than the range of the median parameter sets, so climate model spread and parameter uncertainties are approximately equally important (Fig. 10a-d). For the same period, floods with return periods of 50 years and 100 years shows that the climate model spread is more important than the parameter uncertainty (Fig. 10e-f). During the mid-century, both uncertainties are equally important for floods with return periods of 2 and 5 years (Fig. 10ab), but for the floods with larger return periods (10–100 years) climate model spread is more important than parameter uncertainty (Fig. 10c-f). During the late century, floods with return periods of

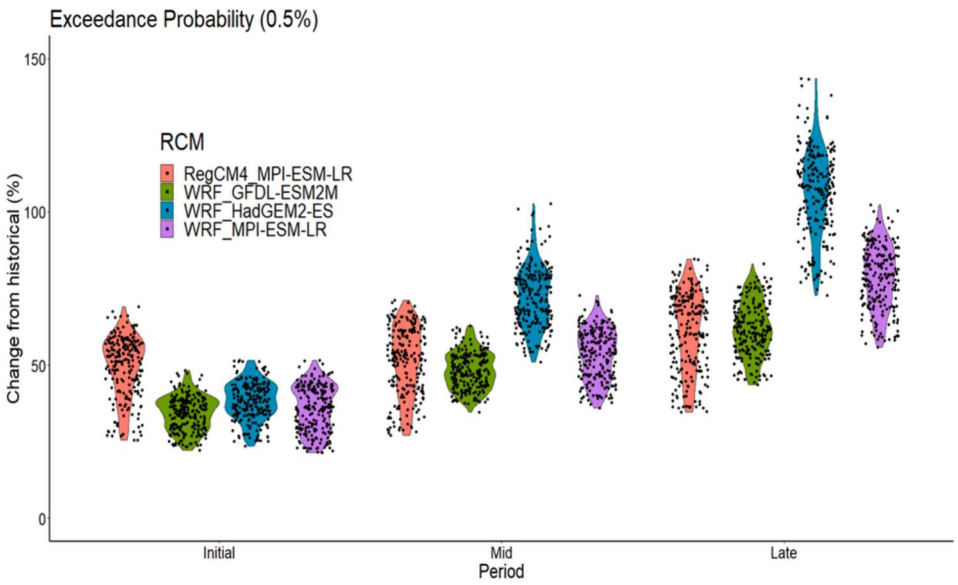

Fig. 7. Percentage change of 0.5% exceedance probability flows as compared to the historical period for all four climate model outputs. This data is extracted from the flow duration curves and each black dot represents output of flow results from one parameter set. The width of the violin plots represents the shape of the distribution, while the black points represent the results from each parameter set. The initial period is 2021–2045, mid is 2046–2070, and late is 2071–2095. Percentage change for 10%, 25%, and 50% flows are shown in Figs. S9–S11.

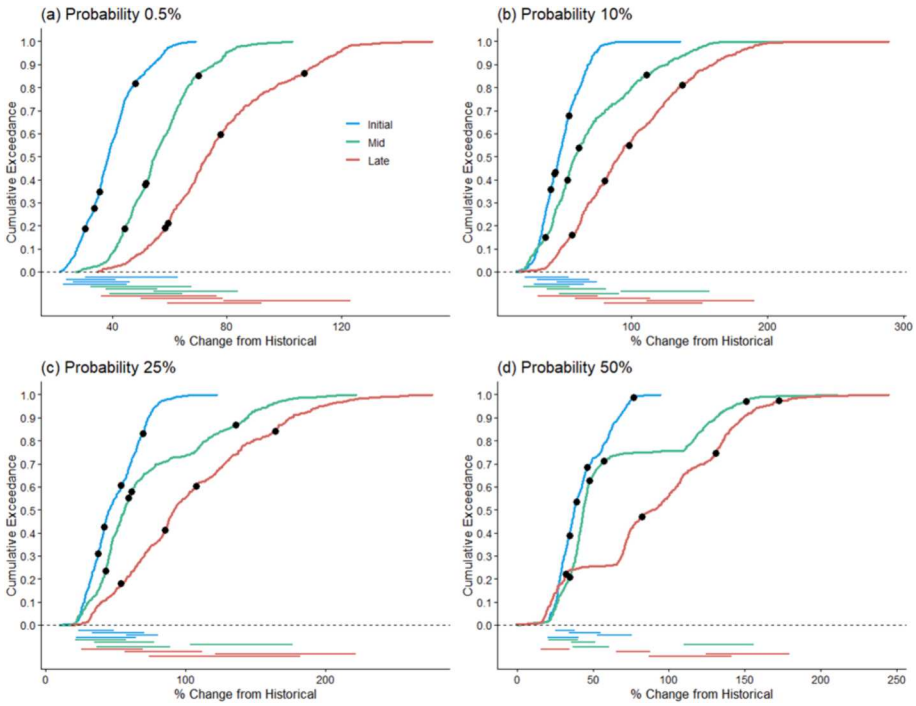

Fig. 8. The cumulative distribution function (CDF) of percentage change of flows as compared to the historical period for all 4 climate models. Each curve represents the data from 896 simulations (224 simulations for each of 4 climate models), while the horizontal lines represent the PI of SWMM results for one climate model. In all panels and for all periods, the PI from RegCM4_MPI-ESM-LR is the top horizontal line, WRF_GFDL-ESM2M is the second line, WRF_HadGEM2-ES is the third line, and WRF_MPI-ESM-LR is the bottom line. The black dots represent the values for the median parameter sets, i.e., those that generate the flow duration curve closest to the median for each climate model in the historical period. The horizontal span of black dots represents the climate model spread for a single calibration. The initial period is 2021–2045, mid is 2046–2070, and late is 2071–2095.

2 and 5 years (Fig. 10ab) showed that the parameter uncertainties are more important than climate model spread, but for the larger return periods 10–100 years, both uncertainties are approximately equally important (Fig. 10c-f).

3.5. *Influence of RCM and GCM on hydrological projections*

The choice of RCMs used in this analysis was limited to CORDEX datasets with 0.22°/25 km spatial resolution and 1 h precipitation outputs. This resulted in two climate projections that had a shared parent GCM MPI-ESM-LR but had differing RCMs (REGCM4 vs. WRF).

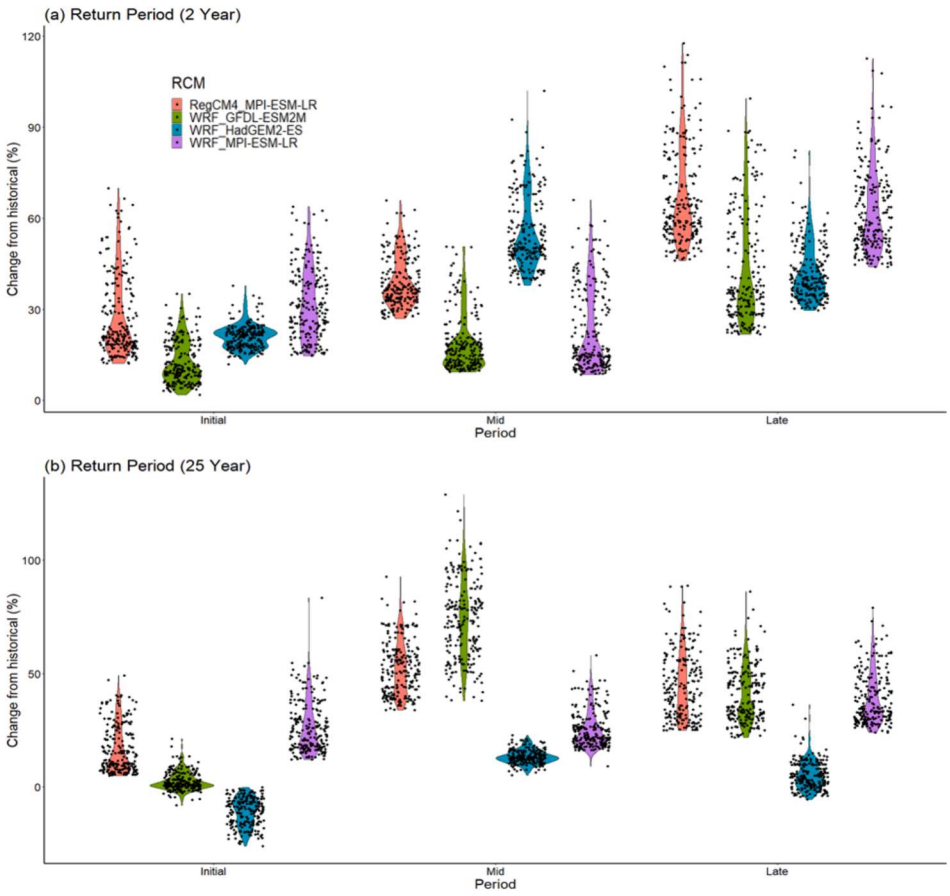

Fig. 9. Percentage change of 2-year and 25-year return period floods as compared to historical for all four climate models. Each black dot represents the percentage change because of one parameter set, and the width of the violin plots represents the shape of the distribution, while the black points represent the results from each parameter set. The initial period is 2021–2045, mid is 2046–2070, and late is 2071–2095. Percentage change for 5-, 10-, 50-, 100-year floods are shown in Figs. S16-S19.

These two climate projections generate similar hydrology during the initial period, but diverge later in the century. Three climate projections used WRF as the RCM, but had differing parent GCMs. When considering a single parameter set, variability among hydrological projections is largest during the late century period for sub-annual flows with 0.5 % to 50 % exceedance probabilities. WRF_HadGEM2-ES projects the largest changes in these flows, aligning with its large projected changes to 6-mo to 1-year precipitation in both 1- and 24-hour storms by the late century. Conversely, three climate projections generate similar projected changes to floods during the late century. WRF_HadGEM2-ES projects the smallest changes to floods, despite producing the largest 24-hour storms with 2- to 10-year return periods. There is greater variability among climate projections in the mid-century period, for both 24-hour storms and floods. Again, WRF_HadGEM2-ES projects a more modest change to floods with $\geq$ 10 years return periods than the other climate models.

4. Discussion

Northeastern Ohio is getting warmer and wetter, leading to a substantial increase in urban streamflow over the 21st century. Despite differences in urbanization and watershed scale from previous studies on flow regime impacts of 21st century climate change in the Great Lakes region, the magnitude of change in West Creek's flow regime is broadly consistent with other regional studies (e.g., Byun et al., 2019; Shrestha et al., 2021). Accepting multiple parameter sets during calibration resulted in a broader range of hydrologic outcomes than was seen across the climate models when only one parameter set was used for SWMM modeling. Overall, uncertainty due to calibration parameters is approximately equally important to climate model spread for projecting changes to future moderate to high flows and floods. As has been previously shown for bias correction decisions (Malek et al., 2022), failure to account for model calibration uncertainties could lead to over- or under-design of critical urban water infrastructure, including bridges, culverts, pipes, and stormwater controls (Cook et al., 2017).

The use of multiple climate models helps constrain confidence in the future flows and floods, by providing an assessment of agreement or spread in projections. Other studies have assessed the importance of RCM versus parent GCM for regional climate change predictions (e.g., Bukovsky and Mearns, 2020). In the study region, climate models may produce varying hydrologic outcomes as a result of their representation of the Great Lakes (Briley et al., 2021) and projections of low level jet dynamics (Zobel et al., 2018), among other differences. Our results show that HadGEM2-ES produces substantially different hydrology than the other models we considered, despite having fairly similar results to the other models in the precipitation depth-duration-frequency analysis. HadGEM2-ES projects more of an increase in summer precipitation, and a higher number of days with precipitation $>$ 25 mm at mid-century, than other climate models (Figs. S21, S22), suggesting that both seasonality and sequencing of heavy precipitation days may contribute to the differences in flow projections, as observed in other systems (e.g., Berghuijs et al., 2016; Ye et al., 2017). Thus, choice of climate model can influence predicted future high flows and floods beyond what is apparent from examination of precipitation depth-duration-frequency curves. Depth-duration frequency analysis was not sufficient to fully identify when climate model spread would be large for modeled flows and floods in continuous simulations. Engineering decisions in urban

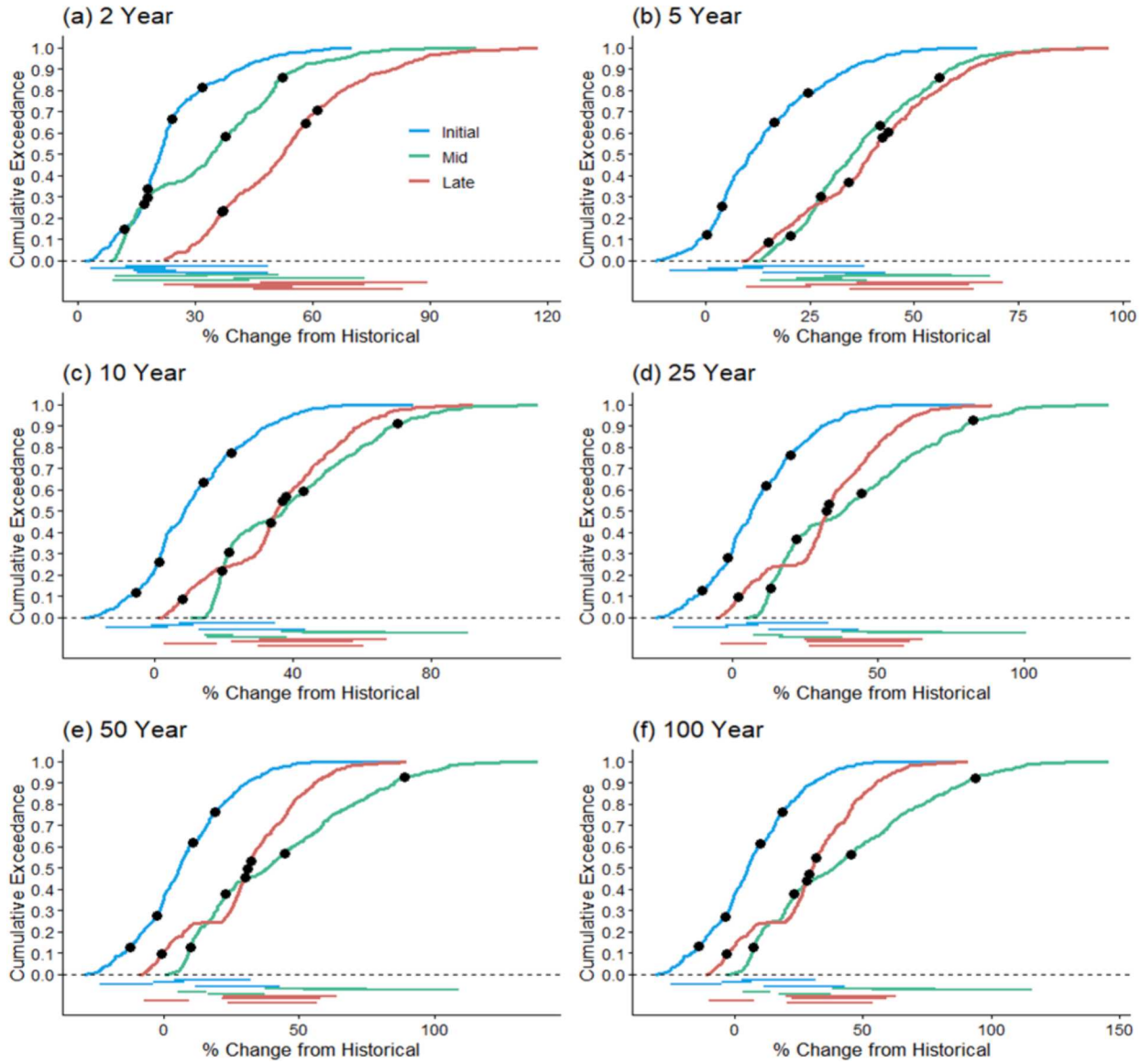

Fig. 10. The cumulative distribution function (CDF) of percentage change of flood frequencies as compared to the historical period for all 4 climate models. Each curve represents the data from 896 simulations (224 simulations for each of 4 climate models), while the horizontal lines represent the PI of SWMM results for one climate model. In all panels and for all periods, the PI from RegCM4_MPI-ESM-LR is the top horizontal line, WRF_GFDL-ESM2M is the second line, WRF_HadGEM2-ES is the third line, and WRF_MPI-ESM-LR is the bottom line. The black dots represent the values for the median parameter sets, i.e., those that generate the flow duration curve closest to the median for each of the 4 climate models in the historical period. The horizontal span of black dots represents the climate model spread for a single calibration. The initial period is 2021–2045, mid is 2046–2070, and late is 2071–2095.

watersheds are often based on depth-duration-frequency curves, which are used to synthesize design storms (e.g., Cook et al., 2017; Grimaldi et al., 2021). However, our results show that analysis of climate change effects based on only design storms could fail to capture the full range of streamflow response, and they suggest there is an important role for continuous streamflow simulations, not just design storms, to inform urban infrastructure decisions in the context of changing precipitation patterns.

Compared to a single calibration, the use of multiple realistic calibration parameters helps capture a much wider range of flows for individual climate models, as well as in aggregate. The comparison of single vs multiple parameters suggests that for sub-annual flows with exceedance probabilities of 0.5–25 %, >30 % of the changes projected by multiple calibrations are outside the range projected by single calibrations from the climate model ensemble. Both upper and lower ends of the CDFs are missed by single calibrations. The impact of calibration parameters is even greater in the case of flood frequency analysis. For these rarer events, we miss 40 % of the CDF generated by multiple calibrations, when using only one calibration per climate model. Here we chose to focus on the median parameter set from a Bayesian calibration approach, and this median parameter set may not be representative of a single "best" calibration using other approaches. Less exhaustive calibration approaches could produce a single parameter set that does not span as wide a range of projected changes as the median parameter set, or they may be biased lower or higher on the CDF. Extrapolating a distribution from four points (one per climate model) could result in over-confidence in a particular projected future (e.g., as seen for 10–100 year floods in the late century, Fig. 10). Thus, choice of a single calibration parameter set could lead to the underestimation of the design parameters for stormwater drainage and flood control infrastructure, similar to the effects seen by (Cook et al., 2020) from RCM resolution and bias correction. Continuous simulations of 100 years of flow using 224 parameter sets is computationally expensive, but it produced a wide range of flows, enabling more robust estimation of

the uncertainties associated with flows and floods with different exceedance probabilities.

When there is relatively good agreement among climate models (e.g., near term flows), hydrologic model calibration uncertainty is particularly important to consider, based on comparison of PI to inter-model spread of the median parameter set. When climate model spread was less than 30–35 % for the four model outputs examined, parameter uncertainty was larger or equally large using the Bayesian model calibration approach employed here. For the West Creek watershed, parameter uncertainty was equally or more important to capture for most near-term (i.e., initial period) moderate to high flows and floods, as well as for late century floods. Conversely, where climate model spread is large, such as during the mid-century for floods or late century for moderate to high flows, parameter uncertainty is relatively less important. To reduce computational expense, a potential approach is to initially use a single calibration to assess climate model spread relative to specific desired hydrologic metrics. If climate model spread is large, Bayesian calibration may not add much value, relative to expense.

A full assessment of all sources of uncertainty in projections of the hydrological impacts of climate change in urban streams is impractical for most engineering applications. Along the cascade of choices from emissions scenario, GCM, downscaling technique, bias correction technique, precipitation disaggregation method, hydrological model selection, and model parameter calibration, we focused on uncertainty arising from the choice of downscaled GCM versus hydrological parameter uncertainty. This choice was motivated by the availability of multiple climate model outputs via NA-CORDEX (Mearns et al., 2017) and Bayesian calibration techniques (e.g., Vrugt, 2016) as putatively accessible to applied hydrologists and by previous work identifying these uncertainty sources as hydrologically important (e.g., Avellaneda and Jefferson, 2020; Feng and Beighley, 2020). Our work builds on previous studies evaluating the effects of GCM spatial and temporal scale, and bias correction techniques on infrastructure design uncertainty (Cook et al., 2020). Unlike some studies in less urban watersheds (e.g., Addor et al., 2014; Feng and Beighley, 2020), we did not compare multiple hydrological models, in part because SWMM is so widely used for urban hydrological applications. Work remains to assess the uncertainty imparted by the precipitation disaggregation (e.g., Müller-Thomy and Sikorska-Senoner, 2019) in the context of other uncertainties in the climate impacts projection cascade, especially in the context of projecting changes to urban floods. Nonetheless, the present work provides guidance on when climate model spread may be most important for uncertainty considerations, when hydrological parameter uncertainty is important, and examples of where caution is needed if parameter uncertainty is not accounted for.

5. Implications and conclusions

By the end of the 21st century, under the RCP8.5 climate change scenario there will be major changes in the hydrology of urban streams in the Great Lakes region, as compared to a 1976–2000 baseline. Projections of increasing future high flows and floods in West Creek suggest that hydrologic changes arising from climate change can potentially lead to infrastructure damage, loss of human lives and ecosystem degradation in urban watersheds. These risks can be minimized by considering climate change in the planning of new infrastructure and management of existing infrastructure, including green stormwater infrastructure, stream restorations, and flood warning systems (e.g., Giese et al., 2019; Perry et al., 2015).

We show that consideration of multiple climate models and hydrological model calibration parameter sets helps capture a wider range of potential climate change impacts on urban streamflow. Quantification of the wide range of uncertainties associated with climate change projections, including those arising from hydrologic model calibration, is helpful to understand the risks of over- or under-estimation of design variables for culverts and bridges, green infrastructure, and other flood mitigation infrastructure in urban watersheds (Lai et al., 2022; Wright et al., 2021).

Results from the SWMM model of West Creek show that where climate model spread is low to moderate, uncertainties related to calibration parameter sets are important. Further, our results demonstrate that ignoring either climate model variability or hydrologic parameter uncertainty could lead to substantial under- or over-estimation of high flow and flood magnitudes. While computationally expensive, a Bayesian calibration approach that accepts multiple realistic parameter sets enables the creation of CDFs of projected flows. These CDFs can be used for data-driven decision making for water resources management that explicitly considers multiple sources of uncertainty.

CRediT authorship contribution statement

Zia Ul Hassan: Writing – review & editing, Writing – original draft, Visualization, Validation, Software, Methodology, Conceptualization. **Anne J. Jefferson:** Writing – review & editing, Visualization, Supervision, Resources, Project administration, Funding acquisition, Conceptualization. **Pedro M. Avellaneda:** Writing – review & editing, Validation, Methodology, Conceptualization. **Aditi S. Bhaskar:** Writing – review & editing, Supervision, Resources, Data curation, Conceptualization.

Declaration of competing interest

The authors declare that they have no known competing financial interests or personal relationships that could have appeared to influence the work reported in this paper.

Data availability

All code is available at Our Hydro share repository at Hassan, Z. U., A. J. Jefferson, P. Avellaneda, A. S. Bhaskar (2024). Assessment of hydrological parameter uncertainty versus climate projection spread on urban streamflow and floods, HydroShare, https://doi.org/10.4211/hs.d43ec15cf9c64b349ca2f3f36de4686b. The repository includes timeseries output for RegCM4_MPI-ESM-LR and all derived data for all RCMs.

Acknowledgments

This material is based upon work supported by the National Science Foundation under Grant No. 1805319. We are grateful to the Northeast Ohio Regional Sewer District (NEORSD) for supplying the uncalibrated SWMM model which is the basis for this work and to NEORSD and Cleveland Metroparks for sharing meteorological data with us. We appreciate the technical support and resources available at the Ohio Supercomputer Center (Ohio Supercomputer Center, 1987). We acknowledge the World Climate Research Programme's Working Group on Regional Climate, and the Working Group on Coupled Modelling, former coordinating body of CORDEX and responsible panel for CMIP5. We also acknowledge the Earth System Grid Federation infrastructure, an international effort led by the U.S. Department of Energy's Program for Climate Model Diagnosis and Intercomparison, the European Network for Earth System Modelling and other partners in the Global Organisation for Earth System Science Portals (GO-ESSP).

Appendix A. Supplementary data

Supplementary data to this article can be found online at https://doi.org/10.1016/j.jhydrol.2024.131546.

References

Addor, N., Rössler, O., Köplin, N., Huss, M., Weingartner, R., Seibert, J., 2014. Robust changes and sources of uncertainty in the projected hydrological regimes of Swiss

catchments. Water Resour. Res. 50, 7541–7562. https://doi.org/10.1002/2014WR015549.
Alamdari, N., Sample, D., Steinberg, P., Ross, A., Easton, Z., 2017. Assessing the effects of climate change on water quantity and quality in an urban watershed using a calibrated stormwater model. Water 9, 464. https://doi.org/10.3390/w9070464.
Alfieri, L., Burek, P., Feyen, L., Forzieri, G., 2015. Global warming increases the frequency of river floods in Europe. Hydrol. Earth Syst. Sci. 19, 2247–2260. https://doi.org/10.5194/hess-19-2247-2015.
Allen, R. G., and Environmental Water Resources Institute, and Task Committee on Standardization of Reference Evapotranspiration The ASCE Standardized Reference Evapotranspiration Equation 2005 Am. Soc. of Civ. Eng Reston, Va.
Aslam, R.A., Shrestha, S., Pal, I., Ninsawat, S., Shanmugam, M.S., Anwar, S., 2020. Projections of climatic extremes in a data poor transboundary river basin of India and Pakistan. Int J Climatol 40, 4992–5010. https://doi.org/10.1002/joc.6501.
Avellaneda, P.M., Jefferson, A.J., Grieser, J.M., Bush, S.A., 2017. Simulation of the cumulative hydrological response to green infrastructure: green infrastructure modeling. Water Resour. Res. 53, 3087–3101. https://doi.org/10.1002/2016WR019836.
Avellaneda, P.M., Jefferson, A.J., 2020. Sensitivity of streamflow metrics to infiltration-based stormwater management networks. Water Resour. Res. 56 https://doi.org/10.1029/2019WR026555.
Barco, J., Wong, K.M., Stenstrom, M.K., 2008. Automatic calibration of the U.S. EPA SWMM model for a large urban catchment. J. Hydraul. Eng. 134, 466–474. https://doi.org/10.1061/(ASCE)0733-9429(2008)134:4(466).
Berghuijs, W.R., Woods, R.A., Hutton, C.J., Sivapalan, M., 2016. Dominant flood generating mechanisms across the United States. Geophys. Res. Lett. 43, 4382–4390. https://doi.org/10.1002/2016GL068070.
Beven, K.J., 2009. Comment on "Equifinality of formal (DREAM) and informal (GLUE) Bayesian approaches in hydrologic modeling?" by Jasper A. Vrugt, Cajo J. F. ter Braak, Hoshin V. Gupta and Bruce A. Robinson. Stoch Environ Res Risk Assess 23, 1059–1060. https://doi.org/10.1007/s00477-008-0283-x.
Bosshard, T., Carambia, M., Goergen, K., Kotlarski, S., Krahe, P., Zappa, M., Schär, C., 2013. Quantifying Uncertainty Sources in an Ensemble of Hydrological Climate-impact Projections. Water Resour. Res. 49 (3), 1523–1536.
Briley, L.J., Rood, R.B., Notaro, M., 2021. Large lakes in climate models: A Great Lakes case study on the usability of CMIP5. Journal of Great Lakes Research 47, 405–418. https://doi.org/10.1016/j.jglr.2021.01.010.
Bukovsky, M.S., Mearns, L.O., 2020. Regional climate change projections from NA-CORDEX and their relation to climate sensitivity. Clim. Change 162, 645–665. https://doi.org/10.1007/s10584-020-02835-x.
Byun, K., Hamlet, A.F., 2018. Projected changes in future climate over the Midwest and Great Lakes region using downscaled CMIP5 ensembles: PROJECTED CLIMATE CHANGES OVER THE MIDWEST AND GREAT LAKES REGION. Int. J. Climatol 38, e531–e553. https://doi.org/10.1002/joc.5388.
Byun, K., Chiu, C.-M., Hamlet, A.F., 2019. Effects of 21st century climate change on seasonal flow regimes and hydrologic extremes over the Midwest and Great Lakes region of the US. Sci. Total Environ. 650, 1261–1277. https://doi.org/10.1016/j.scitotenv.2018.09.063.
Chegwidden, O.S., Nijssen, B., Rupp, D.E., Arnold, J.R., Clark, M.P., Hamman, J.J., Kao, S., Mao, Y., Mizukami, N., Mote, P.W., Pan, M., Pytlak, E., Xiao, M., 2019. How Do Modeling Decisions Affect the Spread Among Hydrologic Climate Change Projections? Exploring a Large Ensemble of Simulations Across a Diversity of Hydroclimates. Earth's Future 7, 623–637. https://doi.org/10.1029/2018EF001047.
Chen, J., Brissette, F.P., Chaumont, D., Braun, M., 2013. Finding appropriate bias correction methods in downscaling precipitation for hydrologic impact studies over North America: Evaluation of Bias Correction Methods. Water Resour. Res. 49, 4187–4205. https://doi.org/10.1002/wrcr.20331.
Chien, H., Yeh, P.-J.-F., Knouft, J.H., 2013. Modeling the potential impacts of climate change on streamflow in agricultural watersheds of the Midwestern United States. J. Hydrol. 491, 73–88. https://doi.org/10.1016/j.jhydrol.2013.03.026.
Clark, M.P., Wilby, R.L., Gutmann, E.D., Vano, J.A., Gangopadhyay, S., Wood, A.W., Fowler, H.J., Prudhomme, C., Arnold, J.R., Brekke, L.D., 2016. Characterizing Uncertainty of the Hydrologic Impacts of Climate Change. Curr Clim Change Rep 2, 55–64. https://doi.org/10.1007/s40641-016-0034-x.
Cook, L.M., Anderson, C.J., Samaras, C., 2017. Framework for Incorporating Downscaled Climate Output into Existing Engineering Methods: Application to Precipitation Frequency Curves. J. Infrastruct. Syst. 23, 04017027. https://doi.org/10.1061/(ASCE)IS.1943-555X.0000382.
Cook, L.M., McGinnis, S., Samaras, C., 2020. The effect of modeling choices on updating intensity-duration-frequency curves and stormwater infrastructure designs for climate change. Clim. Change 159, 289–308. https://doi.org/10.1007/s10584-019-02649-6.
Deletic, A., Dotto, C.B.S., McCarthy, D.T., Kleidorfer, M., Freni, G., Mannina, G., Uhl, M., Henrichs, M., Fletcher, T.D., Rauch, W., Bertrand-Krajewski, J.L., Tait, S., 2012. Assessing uncertainties in urban drainage models. Physics and Chemistry of the Earth, Parts a/b/c 42–44, 3–10. https://doi.org/10.1016/j.pce.2011.04.007.
Feng, D., Beighley, E., 2020. Identifying uncertainties in hydrologic fluxes and seasonality from hydrologic model components for climate change impact assessments. Hydrol. Earth Syst. Sci. 24, 2253–2267. https://doi.org/10.5194/hess-24-2253-2020.
Freer, J., Beven, K., Ambroise, B., 1996. Bayesian Estimation of Uncertainty in Runoff Prediction and the Value of Data: An Application of the GLUE Approach. Water Resour. Res. 32, 2161–2173. https://doi.org/10.1029/95WR03723.
Giese, E., Rockler, A., Shirmohammadi, A., Pavao-Zuckerman, M.A., 2019. Assessing Watershed-Scale Stormwater Green Infrastructure Response to Climate Change in Clarksburg. Maryland. J. Water Resour. Plann. Manage. 145, 05019015. https://doi.org/10.1061/(ASCE)WR.1943-5452.0001099.
Grimaldi, S., Nardi, F., Piscopia, R., Petroselli, A., Apollonio, C., 2021. Continuous hydrologic modelling for design simulation in small and ungauged basins: A step forward and some tests for its practical use. J. Hydrol. 595, 125664 https://doi.org/10.1016/j.jhydrol.2020.125664.
Hamel, P., Daly, E., Fletcher, T.D., 2013. Source-control stormwater management for mitigating the impacts of urbanisation on baseflow: A review. J. Hydrol. 485, 201–211. https://doi.org/10.1016/j.jhydrol.2013.01.001.
Hayhoe, K., Wake, C., Anderson, B., Liang, X.-Z., Maurer, E., Zhu, J., Bradbury, J., DeGaetano, A., Stoner, A.M., Wuebbles, D., 2008. Regional climate change projections for the Northeast USA. Mitig Adapt Strateg Glob Change 13, 425–436. https://doi.org/10.1007/s11027-007-9133-2.
Heineman, Mitchell C. (2004). [American Society of Civil Engineers World Water and Environmental Resources Congress 2004 - Salt Lake City, Utah, United States (June 27-July 1, 2004)] Critical Transitions in Water and Environmental Resources Management - NetSTORM - A Computer Program for Rainfall-Runoff Simulation and Precipitation Analysis. , 1–14. doi:10.1061/40737(2004)395.
Hossain, S., Hewa, G.A., Wella-Hewage, S., 2019. A Comparison of Continuous and Event-Based Rainfall-Runoff (RR) Modelling Using EPA-SWMM. Water 11, 611. https://doi.org/10.3390/w11030611.
Jarden, K.M., Jefferson, A.J., Grieser, J.M., 2016. Assessing the effects of catchment-scale urban green infrastructure retrofits on hydrograph characteristics. Hydrol. Process. 30, 1536–1550. https://doi.org/10.1002/hyp.10736.
Joseph, J., Ghosh, S., Pathak, A., Sahai, A.K., 2018. Hydrologic impacts of climate change: Comparisons between hydrological parameter uncertainty and climate model uncertainty. J. Hydrol. 566, 1–22. https://doi.org/10.1016/j.jhydrol.2018.08.080.
Jung, I.-W., Chang, H., Moradkhani, H., 2011. Quantifying uncertainty in urban flooding analysis considering hydro-climatic projection and urban development effects. Hydrol. Earth Syst. Sci. 15, 617–633. https://doi.org/10.5194/hess-15-617-2011.
Kim, Y., Chester, M. V., Eisenberg, D. A., & Redman, C. L., 2019. The infrastructure trolley problem: Positioning safe-to-fail infrastructure for climate change adaptation. Earth's Future, 7,704–717. https://doi.org/ 10.1029/2019EF001208.
Krysanova, V., Donnelly, C., Gelfan, A., Gerten, D., Arheimer, B., Hattermann, F., Kundzewicz, Z.W., 2018. How the performance of hydrological models relates to credibility of projections under climate change. Hydrol. Sci. J. 63, 696–720. https://doi.org/10.1080/02626667.2018.1446214.
Kundzewicz, Z.W., Krysanova, V., Benestad, R.E., Hov, Ø., Piniewski, M., Otto, I.M., 2018. Uncertainty in climate change impacts on water resources. Environ Sci Policy 79, 1–8. https://doi.org/10.1016/j.envsci.2017.10.008.
Lai, Y., Lopez-Cantu, T., Dzombak, D.A., Samaras, C., 2022. Framing the Use of Climate Model Projections in Infrastructure Engineering: Practices, Uncertainties, and Recommendations. J. Infrastruct. Syst. 28, 04022020. https://doi.org/10.1061/(ASCE)IS.1943-555X.0000685.
Li, M., Yang, X., Sun, B., Chen, L., Shen, Z., 2016. Parameter uncertainty analysis of SWMM based on the method of GLUE. International Proceedings of Chemical, Biological and Environmental Engineering (IPCBEE) 98, 74–79.
Liu, Y., Gupta, H.V., 2007. Uncertainty in hydrologic modeling: Toward an integrated data assimilation framework: HYDROLOGIC DATA ASSIMILATION. Water Resour. Res. 43 https://doi.org/10.1029/2006WR005756.
Luo, M., Liu, T., Meng, F., Duan, Y., Frankl, A., Bao, A., De Maeyer, P., 2018. Comparing Bias Correction Methods Used in Downscaling Precipitation and Temperature from Regional Climate Models: A Case Study from the Kaidu River Basin in Western China. Water 10, 1046. https://doi.org/10.3390/w10081046.
Malek, K., Reed, P., Zeff, H., Hamilton, A., Wrzesien, M., Holtzman, N., Steinschneider, S., Herman, J., Pavelsky, T., 2022. Bias Correction of Hydrologic Projections Strongly Impacts Inferred Climate Vulnerabilities in Institutionally Complex Water Systems. J. Water Resour. Plann. Manage. 148, 04021095. https://doi.org/10.1061/(ASCE)WR.1943-5452.0001493.
L.O. Mearns et al. The NA-CORDEX dataset, version 1.0. NCAR Climate Data Gateway 2017 Boulder CO 10.5065/D6SJ1JCH accessed [30/01/2020].
Mearns, L.O., Gutowski, W., Jones, R., Leung, R., McGinnis, S., Nunes, A., Qian, Y., 2009. A regional climate change assessment program for North America. Eos Trans. AGU 90, 311. https://doi.org/10.1029/2009EO360002.
Meierdiercks, K.L., Smith, J.A., Baeck, M.L., Miller, A.J., 2010. Analyses of Urban Drainage Network Structure and its Impact on Hydrologic Response [1]. J American Water Resour Assoc 46, 932–943. https://doi.org/10.1111/j.1752-1688.2010.00465.x.
Mendoza, P.A., Clark, M.P., Mizukami, N., Newman, A.J., Barlage, M., Gutmann, E.D., Rasmussen, R.M., Rajagopalan, B., Brekke, L.D., Arnold, J.R., 2015. Effects of Hydrologic Model Choice and Calibration on the Portrayal of Climate Change Impacts. J. Hydrometeorol. 16, 762–780. https://doi.org/10.1175/JHM-D-14-0104.1.
Moore, T.L., Gulliver, J.S., Stack, L., Simpson, M.H., 2016. Stormwater management and climate change: vulnerability and capacity for adaptation in urban and suburban contexts. Clim. Change 138, 491–504. https://doi.org/10.1007/s10584-016-1766-2.
Muleta, M.K., McMillan, J., Amenu, G.G., Burian, S.J., 2013. Bayesian Approach for Uncertainty Analysis of an Urban Storm Water Model and Its Application to a Heavily Urbanized Watershed. J. Hydrol. Eng. 18, 1360–1371. https://doi.org/10.1061/(ASCE)HE.1943-5584.0000705.
Müller-Thomy, H., Sikorska-Senoner, A.E., 2019. Does the complexity in temporal precipitation disaggregation matter for a lumped hydrological model? Hydrol. Sci. J. 64, 1453–1471. https://doi.org/10.1080/02626667.2019.1638926.
Nayeb Yazdi, M., Ketabchy, M., Sample, D.J., Scott, D., Liao, H., 2019. An evaluation of HSPF and SWMM for simulating streamflow regimes in an urban watershed.

Environ. Model. Softw. 118, 211–225. https://doi.org/10.1016/j.envsoft.2019.05.008.
Naz, B.S., Kao, S.-C., Ashfaq, M., Rastogi, D., Mei, R., Bowling, L.C., 2016. Regional hydrologic response to climate change in the conterminous United States using high-resolution hydroclimate simulations. Global Planet. Change 143, 100–117. https://doi.org/10.1016/j.gloplacha.2016.06.003.
O'Donnell, E.C., Thorne, C.R., 2020. Drivers of future urban flood risk. Phil. Trans. r. Soc. a. 378, 20190216. https://doi.org/10.1098/rsta.2019.0216.
Olds, H.T., Corsi, S.R., Dila, D.K., Halmo, K.M., Bootsma, M.J., McLellan, S.L., 2018. High levels of sewage contamination released from urban areas after storm events: A quantitative survey with sewage specific bacterial indicators. PLoS Med 15, e1002614.
Ormsbee, L.E., 1989. Rainfall Disaggregation Model for Continuous Hydrologic Modeling. J. Hydraul. Eng. 115, 507–525. https://doi.org/10.1061/(ASCE)0733-9429(1989)115:4(507).
Pang, X., Gu, Y., Launiainen, S., Guan, M., 2022. Urban hydrological responses to climate change and urbanization in cold climates. Sci. Total Environ. 817, 153066 https://doi.org/10.1016/j.scitotenv.2022.153066.
Perin, R., Trigatti, M., Nicolini, M., Campolo, M., Goi, D., 2020. Automated calibration of the EPA-SWMM model for a small suburban catchment using PEST: a case study. Environ Monit Assess 192, 374. https://doi.org/10.1007/s10661-020-08338-7.
Perry, L.G., Reynolds, L.V., Beechie, T.J., Collins, M.J., Shafroth, P.B., 2015. Incorporating climate change projections into riparian restoration planning and design. Ecohydrology 8, 863–879. https://doi.org/10.1002/eco.1645.
Pyke, C., Warren, M.P., Johnson, T., LaGro, J., Scharfenberg, J., Groth, P., Freed, R., Schroeer, W., Main, E., 2011. Assessment of low impact development for managing stormwater with changing precipitation due to climate change. Landsc. Urban Plan. 103, 166–173. https://doi.org/10.1016/j.landurbplan.2011.07.006.
Revi, A., D.E. Satterthwaite, F. Aragón-Durand, J. Corfee-Morlot, R.B.R. Kiunsi, M. Pelling, D.C. Roberts, and W. Solecki, 2014: Urban areas. In: Climate Change 2014: Impacts, Adaptation, and Vulnerability. Part A: Global and Sectoral Aspects. Contribution of Working Group II to the Fifth Assessment Report of the Intergovernmental Panel on Climate Change.
Rosenzweig, B., Ruddell, B.L., McPhillips, L., Hobbins, R., McPhearson, T., Cheng, Z., Chang, H., Kim, Y., 2019. Developing knowledge systems for urban resilience to cloudburst rain events. Environ Sci Policy 99, 150–159. https://doi.org/10.1016/j.envsci.2019.05.020.
Rossman, L.A., 2010. Storm water management model user's manual, version 5.0. In: Cincinnati: National Risk Management Research Laboratory, Office of Research and Development. US Environmental Protection Agency, p. (p. 276)..
Schoups, G., Vrugt, J.A., 2010. A formal likelihood function for parameter and predictive inference of hydrologic models with correlated, heteroscedastic, and non-Gaussian errors. Water Resour. Res. 46, 2009WR008933 https://doi.org/10.1029/2009WR008933.
Shahed Behrouz, M., Zhu, Z., Matott, L.S., Rabideau, A.J., 2020. A new tool for automatic calibration of the storm water management model (SWMM). J. Hydrol. 581, 124436 https://doi.org/10.1016/j.jhydrol.2019.124436.
Sharma, A., Hamlet, A.F., Fernando, H.J.S., Catlett, C.E., Horton, D.E., Kotamarthi, V.R., Kristovich, D.A.R., Packman, A.I., Tank, J.L., Wuebbles, D.J., 2018. The Need for an Integrated Land-Lake-Atmosphere Modeling System, Exemplified by North America's Great Lakes Region. Earth's Future 6, 1366–1379. https://doi.org/10.1029/2018EF000870.
Shrestha, S., Sharma, S., 1. Civil and Environmental Consultants Inc, Bridgeport, WV 26554, USA, 2. Civil/Environmental Engineering Program, Youngstown State University, One University Plaza, Youngstown, OH 44555, USA, 2021. Assessment of climate change impact on high flows in a watershed characterized by flood regulating reservoirs. Int. J. Agric. Biol. Eng. 14, 178–191. https://doi.org/10.25165/j.ijabe.20211401.5883.
Steinschneider, S., Polebitski, A., Brown, C., Letcher, B.H., 2012. Toward a statistical framework to quantify the uncertainties of hydrologic response under climate change: HYDROLOGIC ALTERATION UNDER CLIMATE CHANGE. Water Resour. Res. 48 https://doi.org/10.1029/2011WR011318.
Sytsma, A., Bell, C., Eisenstein, W., Hogue, T., Kondolf, G.M., 2020. A geospatial approach for estimating hydrological connectivity of impervious surfaces. J. Hydrol. 591, 125545 https://doi.org/10.1016/j.jhydrol.2020.125545.
Turner, V.K., Jarden, K., Jefferson, A., 2016. Resident perspectives on green infrastructure in an experimental suburban stormwater management program 34.
Voskamp, I.M., Van de Ven, F.H.M., 2015. Planning support system for climate adaptation: Composing effective sets of blue-green measures to reduce urban vulnerability to extreme weather events. Build. Environ. 83, 159–167. https://doi.org/10.1016/j.buildenv.2014.07.018.
Vrugt, J.A., 2016. Markov chain Monte Carlo simulation using the DREAM software package: Theory, concepts, and MATLAB implementation. Environ. Model. Softw. 75, 273–316. https://doi.org/10.1016/j.envsoft.2015.08.013.
Wang, M., Zhang, D.Q., Su, J., Trzcinski, A.P., Dong, J.W., Tan, S.K., 2017. Future Scenarios Modeling of Urban Stormwater Management Response to Impacts of Climate Change and Urbanization. Clean - Soil, Air, Water 45, 1700111. https://doi.org/10.1002/clen.201700111.
Wang, M., Zhang, D., Cheng, Y., Tan, S.K., 2019. Assessing performance of porous pavements and bioretention cells for stormwater management in response to probable climatic changes. J. Environ. Manage. 243, 157–167. https://doi.org/10.1016/j.jenvman.2019.05.012.
Wilson, A.B., J.M. Baker, E.A. Ainsworth, J. Andresen, J.A. Austin, J.S. Dukes, E. Gibbons, B.O. Hoppe, O.E. LeDee, J. Noel, H.A. Roop, S.A. Smith, D.P. Todey, R. Wolf, and J.D. Wood, 2023: Ch. 24. Midwest. In: Fifth National Climate Assessment. Crimmins, A.R., C.W. Avery, D.R. Easterling, K.E. Kunkel, B.C. Stewart, and T.K. Maycock, Eds. U.S. Global Change Research Program, Washington, DC, USA. https://doi.org/10.7930/NCA5.2023.CH24.
Wright, D.B., Bosma, C.D., Lopez-Cantu, T., 2019. U.S. Hydrologic Design Standards Insufficient Due to Large Increases in Frequency of Rainfall Extremes. Geophys. Res. Lett. 46, 8144–8153. https://doi.org/10.1029/2019GL083235.
Wright, D.B., Samaras, C., Lopez-Cantu, T., 2021. Resilience to Extreme Rainfall Starts with Science. Bull. Am. Meteorol. Soc. 102, E808–E813. https://doi.org/10.1175/BAMS-D-20-0267.1.
Ye, S., Li, H.-Y., Leung, L.R., Guo, J., Ran, Q., Demissie, Y., Sivapalan, M., 2017. Understanding Flood Seasonality and Its Temporal Shifts within the Contiguous United States. J. Hydrometeorol. 18, 1997–2009. https://doi.org/10.1175/JHM-D-16-0207.1.
Zahmatkesh, Z., Karamouz, M., Nazif, S., 2015. Uncertainty based modeling of rainfall-runoff: Combined differential evolution adaptive Metropolis (DREAM) and K-means clustering. Adv. Water Resour. 83, 405–420. https://doi.org/10.1016/j.advwatres.2015.06.012.
Zhou, Q., Leng, G., Su, J., Ren, Y., 2019. Comparison of urbanization and climate change impacts on urban flood volumes: Importance of urban planning and drainage adaptation. Sci. Total Environ. 658, 24–33. https://doi.org/10.1016/j.scitotenv.2018.12.184.
Zobel, Z., Wang, J., Wuebbles, D.J., Kotamarthi, V.R., 2018. Analyses for high-resolution projections through the end of the 21st century for precipitation extremes over the United States. Earth's Future 6 (10), 1471–1490.